International Research Journal of Engineering and Technology (IRJET) e-ISSN: 2395-0056
Volume: 05 Issue: 11 | Nov 2018 www.irjet.net p-ISSN: 2395-0072

Off-Axis Motor Overdrive Ducted Fan

Abhilekh Mukherjee

MSc, Department of Aerospace Engineering, University of Southampton, Southampton, SO171BJ, UK

Abstract - *The ability of a ducted fan UAV to hover and fly at high speed is a key advantage when proximity to a target is essential. The purpose of this research paper is to design a patent pending [22] modular 3d printed ducted fan with main objectives of improving the stator and implementing a high efficiency low kV brushless motor to replace the conventional high kV motor in an off-axis pattern with an overdrive transmission to improve the abrupt flow separation and swirl in slipstream of the fan contributing to increased axial velocity component and hence more thrust. The designs of modular conventional and off-axis ducted fans are carried with focus on FEA followed by CFD analysis. A conventional on-axis motor ducted fan is compared with the off-axis version in terms of thrust, drag and power and efficiency. The manufactured 3d printed ducted fans are tested in a wind tunnel and the CFD results are compared.*

Key Words: **UAV; off-axis ducted fan; over-drive transmission; swirl; FEA; CFD;**

1. INTRODUCTION

The *FEEG2001 UAV* [23] is a low-cost, 1.5 kg UAV powered by an 1800 mAh 40C Lithium polymer battery and it relies on a 64 mm electric ducted fan for propulsion. So far *Emma* [1], *Ignacio* [2], *Robie* [3], *Nathan* [4] tried to improve the nacelle, stators, and fan geometries in their respective projects. With reduction in drag from the nacelle and with improved stators a bigger aspect of the ducted fan itself was ignored, that is the influence of the motor on the slipstream of the fan and the resultant thrust.

A few references from a handful experiments and simulations conducted have aided in design selection and computational model selection in this research paper.

The following Patents relate to the field of the invention as prior art:

US 5,820,345 (13-10-1998; Abstract, Fig. 3, Summary, Claim 1, 2&8): The invention compares a 'known' co-rotating two stage *SDLF* to the claimed Split Rotor Shaft Driven Lift Fan. The current research relates to a gear transmission with an off-axis mounted motor for low torque high speed operation (varied through a plurality each of spur and bevel gears) as opposed to existing constant speed and torque transmission.

US 2009/0155060A1 (Published 18-06-2009; Page 1 Para 004 & 0011, Claim 4): The invention relates to a centrifugal pump where the inventor has coined the term 'Diffuser' to stator with a generic aerofoil shape which is claimed to reduce swirl, act as a heat exchanger and improve the centrifuge of the fan. However, the current research relates to an asymmetric stator geometry with blade aerofoil i.e. *NACA* 0012 & 0024 at angle of incidence range of 15^0 to 25^0 in the slipstream of the ducted fan to reduce swirl and increase efficiency. The asymmetry of the present stator configuration is to accommodate the off-axis gear transmission.

Experiments conducted by *Abrego* [16] and *Graf* [5] have proved instrumental in designing the stator for the off-axis duct system. *Graf* [5] extensively performed vane effectiveness study across a range of control vane deflection angle from -30° to +30° in 5° increments. He quotes deflection angles outside of the range from +20° to -25° displayed little improvement in pitching moment control due to flow separation illustrated by tuft flow visualisation on the control vane.

Abrego [16] [17], performed experiments on an anti-clockwise rotating fan. It is observed that vane effectiveness does not improve significantly beyond -20° despite a larger chord flap. Control vane effectiveness in both the experiments link to effective lift generation on the control surfaces resulting in moment about the axis of the ducted fan unit. Drop in this effectiveness with large deflection angles means reduced lift and increased drag from flow separation. For the present research paper the stator design and pitch angle are inspired by the control vane design and study involved in the above two papers.

Carlos [18] conducted experiment on wind turbine fairing geometries on upstream tower and found that for *Re* of 6.82e4 the fractional lift loss due to wake from the tower is lowest in E863r45 (E863r series is designed by forcing a thickness ratio of 0.4 and 0.45 by rounding trailing edge). The fairing designs for comparable *Re* are decided upon from the conclusions drawn in the above paper.

Rezaeiha et al. [14] studied the effect of the shaft on the aerodynamic performance of *VAWT*'s with a wide range of δ_{shaft} (shaft-to-turbine diameter ratio). They concluded that the reduction in C_P (power coefficient) increases asymptotically from 0 to 5.5% for δ_{shaft} from 0 to 16%. They also noted that the impact of the shaft-to-turbine rotational speed ratio on the performance of the turbine is negligible. A conclusion is therefore drawn to not expose the transmission shaft in the off-axis ducted fan in the present project. Instead one of the stator vanes with recess is used to pass the transmission shaft through to avoid interaction of the shaft with the slipstream of the fan.

The torque available increases with the cube of the diameter and essentially for a low speed motor the required drive current is lower and hence the conduction losses are reduced which increases the motor efficiency. For the off-axis duct system a low 850 *kV* 41.8 mm diameter pancake motor is chosen over the existing 3500 *kV* 28 mm diameter motor.

Akturk [7] studied tip clearance losses and defined *FFP* for forward flight. The qualitative shape of the loss curves in span wise direction of 3.6% tip clearance shroud was very similar to that of 5.8% clearance. However, the hub and tip region *FFP* were lower in shroud with 3.6% than 5.8% tip clearance. Hence a reasonable inference is made and a tip clearance of 4.6% is chosen for the paper.

Konstantinos [13], *Rezaeiha et al.* [14], *Marcelo et al.* [11] and *Bardina et al.* [6] validated the robustness of *k-ω SST* model in predicting complex flows involving separation while simultaneously being comparable with best models for simple flows. The current computational study uses *k-ω SST* model for simulations of an incompressible mean flow field around a 64 mm ducted fan where the rotor tip Mach number is 0.1849 for 20,000 *RPM* for which compressibility effects are not significant.

2. DESIGNING

As per *Petro* [15] conduction losses decreases with physical motor size. As such for the off-axis duct system an *Avionic 3506 - 850KV* 41.8 mm diameter pancake motor is chosen over the existing *HK2627 EDF Outrunner 4300kV* 28 mm diameter motor. Theoretically the maximum achievable torque (Nm) of a motor is given by equation (1):

$$\tau_{max} = \frac{P_{max}}{2\pi\nu_{max}} \qquad (1)$$

Where P_{max} is the maximum input power (W) and ν_{max} is the maximum achievable angular frequency (rad/s). The available torque in the off-axis motor is changeable with a modular gear configuration mentioned in *Table 2.* Maximum achievable torque for the on-axis and off-axis with two gear configurations are calculated based on maximum operating voltage of 14.8 V and are presented in *Table 1.*

***Table 1**: Maximum available torque*

	Torque (Nm)
$\tau_{max,\ on\text{-}axis}$	0.099
$\tau_{max,\ config\ I}$	0.103
$\tau_{max,\ config\ II}$	0.077

It is decided to use a conventional duct with 1.5 mm wall thickness and not venture into possibilities of improving the design for better performance characteristics. To effectively model and simulate the fan an already 3D scanned (taken using 3Shape Q800 Scanner and a high-resolution 3D scanner) and parameterised model is used.

The stator vane design is frozen for both on-axis and off-axis duct units for easy comparison of performance parameters. It is decided to use four stator vanes and not venture into optimizing the stator vane count.

	Hub	Mid span	Tip
β_1	50°	40°	20°
β_2	40°	35°	30°
Blade chord (in mm)	14.23	13.2	9.86

	mm
Rotor hub diameter	28
Rotor tip diameter	60.6
Rotor blade span	16.3
Max. blade thickness	1.5
Shroud inner diameter for 4.5% tip clearance	31.75

***Table 2**: Geometric specification of 64 mm ducted fan*

From the inference drawn from *Rezaeiha et al.* [14] the transmission shaft is decided to be passed through one of the stator vanes. The transmission shaft with 2 mm diameter plays a crucial role in deciding on an asymmetric stator configuration. Three NACA 0012 aerofoils and one NACA 0024 aerofoil for the transmission shaft to pass through are chosen for the stator vanes. The stator vane chord is kept constant at 15 mm compared to the blade chords in *Table 2*.

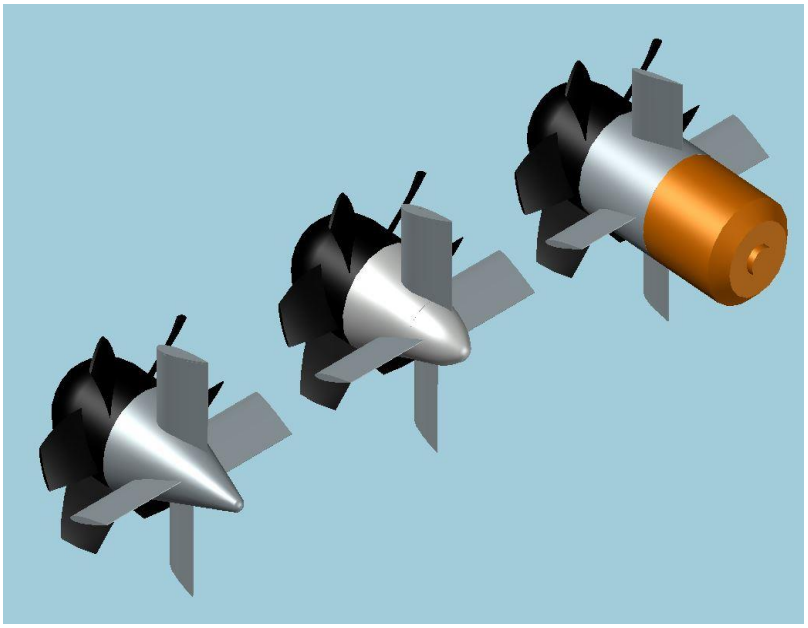

***Figure 1**: Stator configurations: on-axis (right); snub (middle); conical (left)*

Three stator configurations are designed, on-axis with constant hub radius, snub and conical. The **on-axis** configuration is designed to accommodate the motor hence a constant radius of 14 mm is chosen throughout the hub geometry. The off-axis **snub** configuration is designed to accommodate the snub bevel gearbox (*Figure 1*) necessitated by the off-axis positioning of the motor away from the fan. It has an overall length of 33 mm and a slope of 0.424 with a splined tip. The off-axis **conical** configuration is designed for a conical bevel gearbox the same way as **snub**, however, a relaxed slope of 0.368 is chosen with a length of 38 mm and a narrow tip.

The off-axis configuration of the motor necessitated a bevel gearbox with a gear ratio of 1:1 (driving gear: driven gear) to transfer power from the transmission shaft to the fan. The gearbox design should be such that it could be accessed for gear lubrication or replacement. Hence it is decided to slice the gearbox into two volumes with four pairs of M1.7 screws and nuts

securing them in position. The ***3 mm shaft*** is secured in place by two bearings, *MR84ZZ* and *MR63ZZ*. This is so because the variable radius of the bearings helps secure the shaft in position from the axial forces developed by the fan. Also the driving gear has an *OD* of 4 mm which is compatible with *MR84ZZ.* The ***2 mm shaft*** is essentially the transmission shaft which passes through one of the stators and transfers power to the bevel gearbox. This shaft is thinner than the fan shaft so as to allow it to be transmitted through the NACA 0024 stator vane and have enough clearance for rotation. This shaft is held in place with three *MR52ZZ* bearings. Two of such bearings are housed in each split volume of the gearbox on an inclined plane of 45° (*Figure 2*) and the third one lies on the edge of the duct wall leading to the modular spur gearbox.

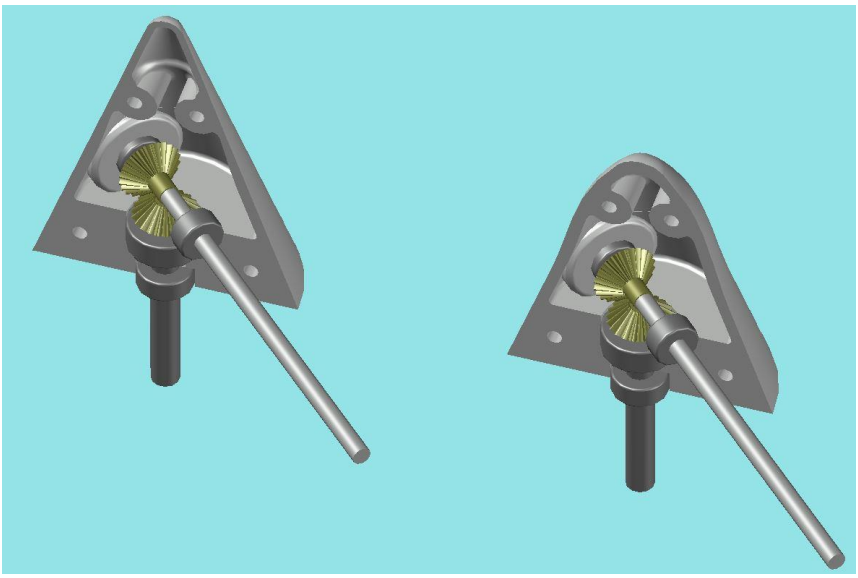

Figure 2*: Sliced perspective view of conical and snub bevel gearboxes*

Table 3*: Specifications for straight bevel gear design in Solidworks (units in mm)*

Module	0.5
Teeth count	14
Pinion's teeth count	14
Pressure angle	20
Face width	2.8
Hub diameter	4
Mounting distance	8
Nominal shaft diameter	3

The ***on-axis*** duct design is a union of the basic duct and the on-axis stator with recesses for M2 nuts to hold the mount which is then supported in the wind tunnel by two M6 screws. This duct is, however, a single unit (*Figure 3*) as the on-axis motor could be screwed on and off the mount by sliding along the set of guide rails provided within the motor mount.

The gearbox is sliced in 45° plane angle with respect to horizontal such that the ***off-axis*** duct also must be able to be taken apart and screwed back again for access to internal bevel gearbox. As such a 45° slicing plane is also chosen to slice the duct into two volumes and care is taken so as to stop the two units from warping and get misaligned from axial forces and mechanical vibrations.

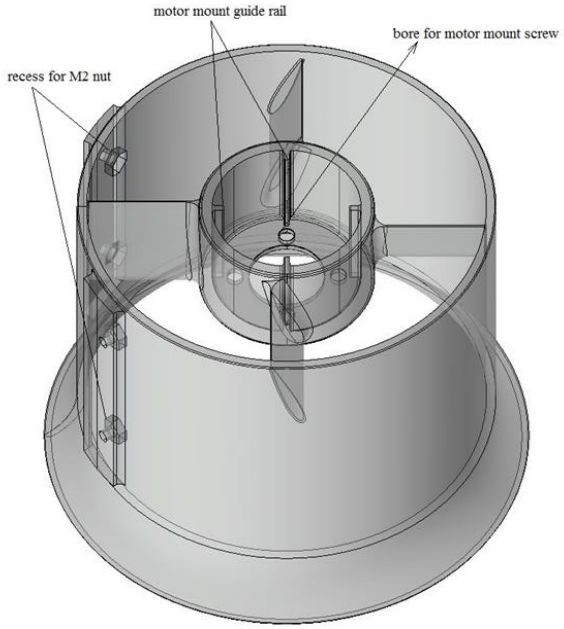

***Figure 3**: X-Ray view of modular on-axis duct*

A sliding rail pair on each sliced volume mates with the other pair on the other unit. With recess for four pairs of M2 screws and nuts, this design ensures that both the volumes anchor well together. Also recess for four other nuts are provided in one of the sliced duct volume to hold the motor-spur gearbox mount. A recess for one MR52ZZ bearing is provided (*Figure 4*) to hold the third bearing of the bevel gearbox supporting the transmission shaft.

A modular gear ratio is one of the design aspects of the current research paper. For the motor to be able to power the fan with optimal torque in an overdrive transmission configuration the design of the ***motor-spur gearbox mount*** is made such that the motor could be slid along to accommodate variable spur gears with variable gear teeth count. A sliding room of 2 mm (*Figure 6*) in the bores to hold the motor screws is provided to support spur gears of variable radius.

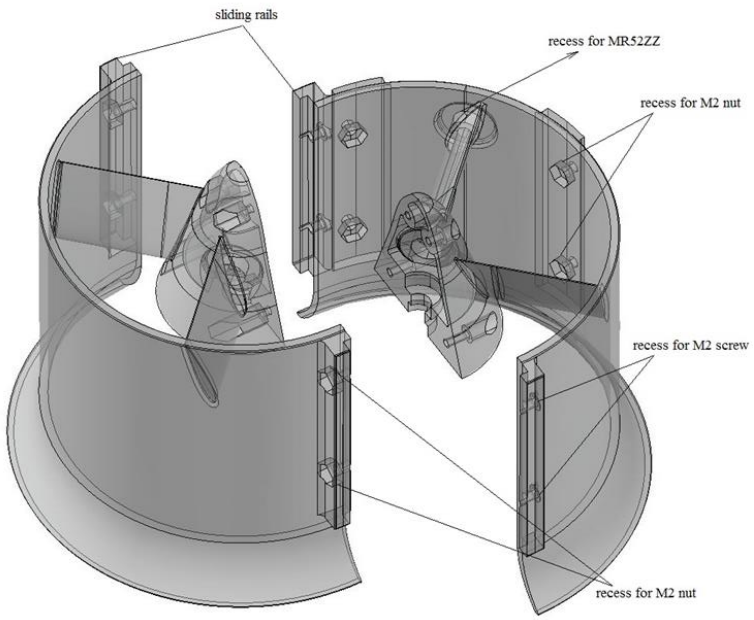

***Figure 4**: X -Ray view of modular off-axis duct with snub gearbox*

***Table 4**: Modular spur gearbox configuration RPM*

configuration I		configuration II	
gear type	*RPM*	gear type	*RPM*
30T spur gear	13	40T spur gear	13
pinion gear	30	pinion gear	40
driving gear	30	driving gear	40
driven gear	30	driven gear	40

***Figure 5**: Motor-spur gearbox mount*

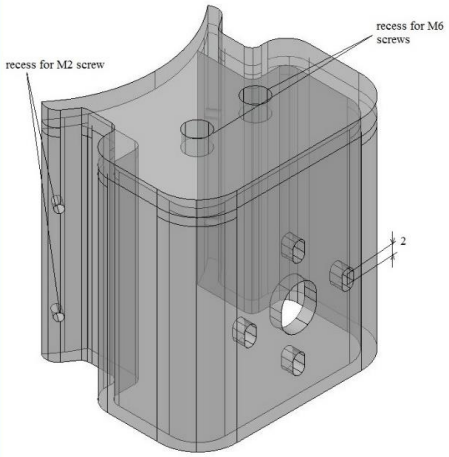

***Figure 6**: X-Ray view of motor-spur gearbox mount in a different perspective*

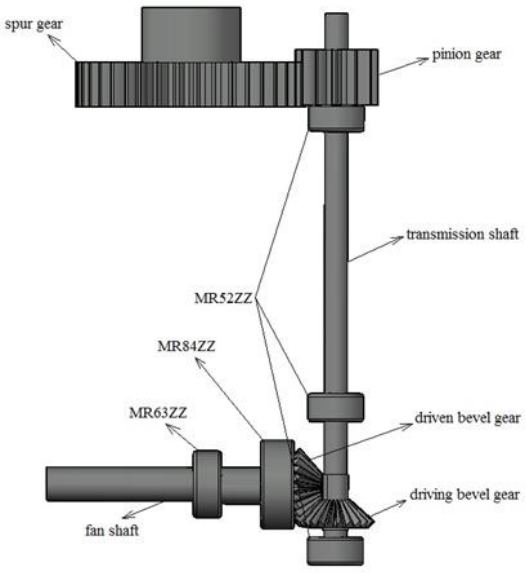

***Figure 7**: Gear transmission layout*

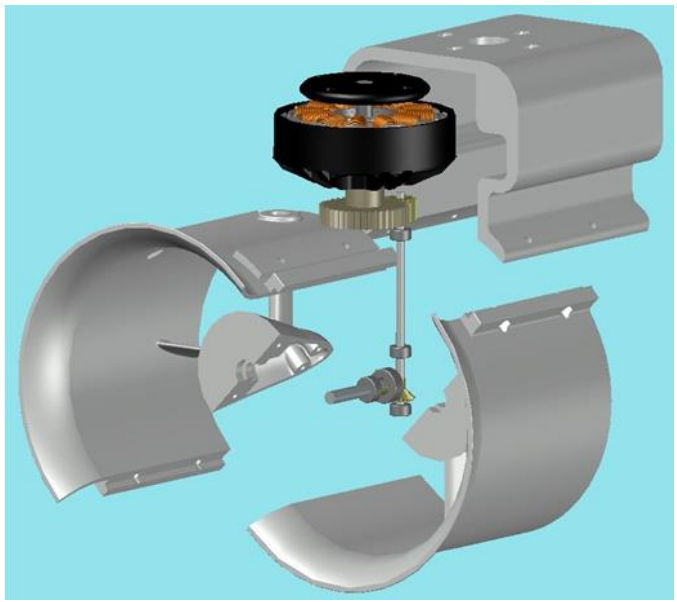

***Figure 8**: Exploded CAD assembly of the off- axis duct*

3. FINITE ELEMENT ANALYSIS

Finite element analysis of any component in an experiment is instrumental in understanding its structural abilities before actually plugging it up and risk parts falling apart or thrown off. *FEA* is performed on all the three duct configurations using material properties of *sintered laser nylon 12* and the boundary conditions with maximum possible magnitude of forces and moments as presented in *Table 5* and illustrated in *Figure 9*. Total deformation and Von-Mises stresses on all the three configurations are noted in *Table 6* and a few are illustrated in *Figure 9* and *Figure 10.* Greater stress concentration at the root of stator vane of conical gearbox design is noted.

***Table 5**: Laser 12 structural properties (left); Forces and moments acting on ducted fan (right)*

Elastic Modulus	1700 MPa	Thrust	9 N
Poisson's Ratio	0.393999	Fan moment	0.3 Nm
Mass Density	930 kg/m3	Motor moment	0.112 Nm
Yield Strength	58 MPa		

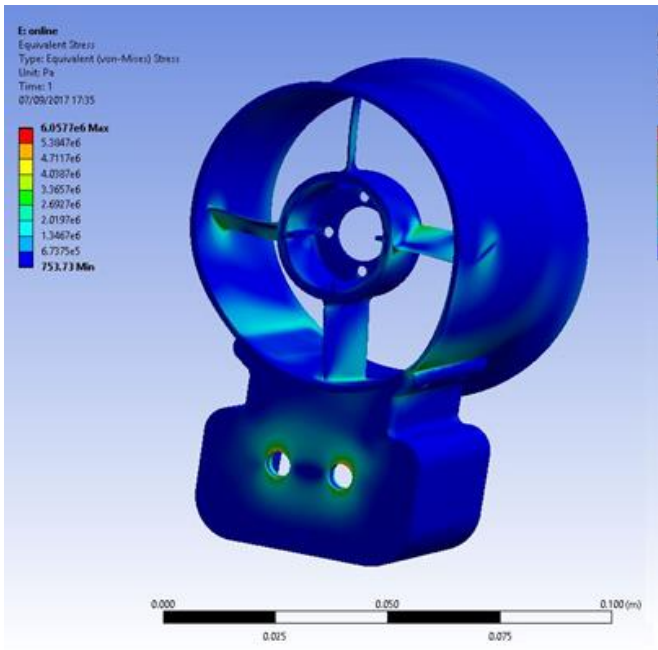

***Figure 9**: Von-Mises stress contour of on-axis design (exaggerated 16x)*

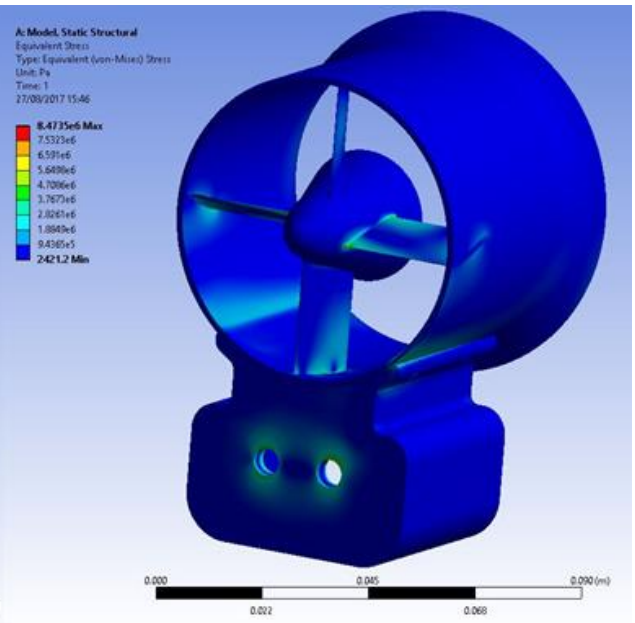

***Figure 10**: Von-Mises stress contour of off-axis snub design (exaggerated 16x)*

Table 6: *FEA results*

	on-axis duct	snub gearbox duct	conical gearbox duct
Total deformation (mm)	0.69	0.675	0.68
Von-Mises stress (MPa)	6.057	8.4	8.8

4. COMPUTATIONAL FLUID DYNAMICS ANALYSIS

Elaborate *CFD* using the modified time-averaged version of *Navier-Stokes* equation called the *Reynolds Averaged Navier-Stokes* (*RANS*) equation is used with the *k-ω SST* model with low Reynold's correction combining both the *k-ω* and *k-ε* with fair accuracy along with low *Re* correction which is essential for the current simulation where the *Re* is found to be approximately 65,000. A few illustrations of the *CFD* analysis are presented in *Figure 11* and *Figure 12.*

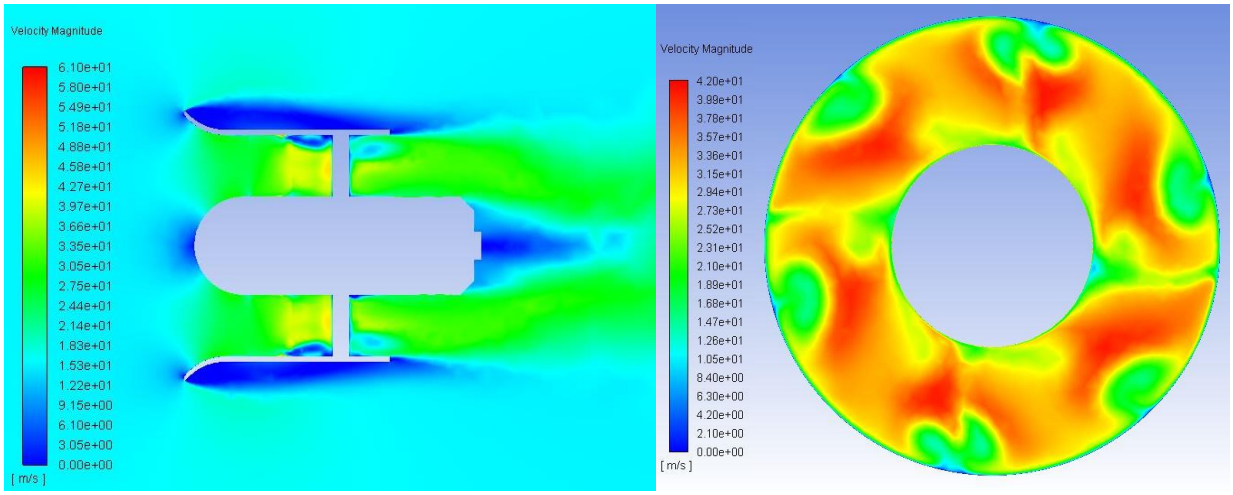

Figure 11*: Conventional motor ducted fan at 18 m/s (not to scale): Velocity contour on slicing plane (left); Velocity contour on iso-clip (right)*

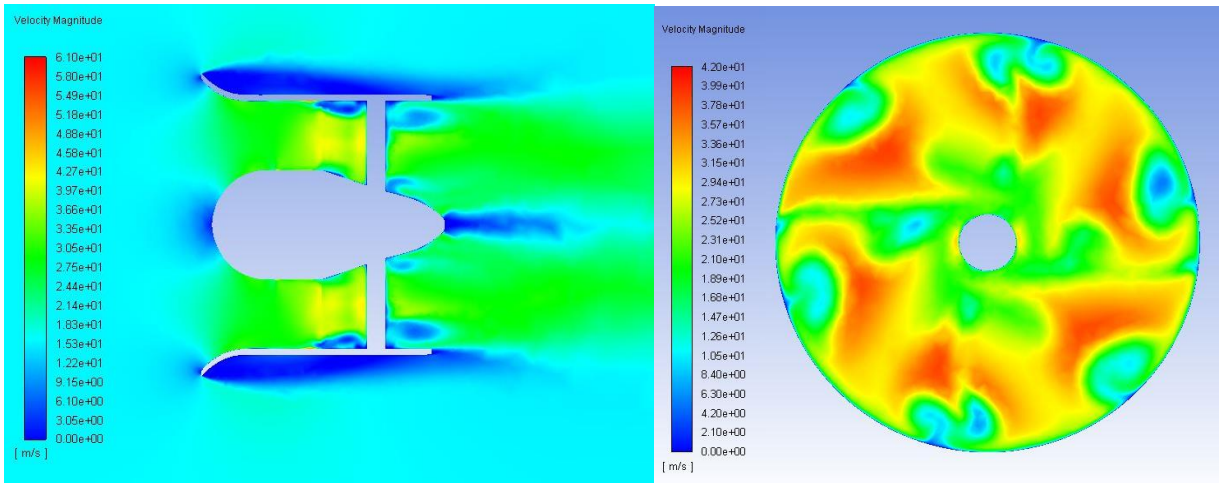

Figure 12*: Snub gearbox ducted fan at 18 m/s (not to scale): Velocity contour on slicing plane (left); Velocity contour on iso-clip (right)*

The flow associated with ducted fans are turbulent in nature with significant amount of swirl. The strength of the swirl is gauged by the swirl number S_n, defined as the ratio of the axial flux of angular momentum to the axial flux of the axial momentum. Equation (2) is used extensively in comparing the flow quality leaving the several configurations of ducted fans.

$$S_n = \frac{2\iint \rho u_\theta r^2 dA}{D\iint \rho u_x^2 r dA} \qquad (2)$$

Where ρ is the air density in room temperature, u_x is the axial component of velocity, u_ϑ is the tangential component of velocity, D is the effective duct inner diameter, r is fan radius and dA is the elemental surface area on the surface the Swirl number is evaluated.

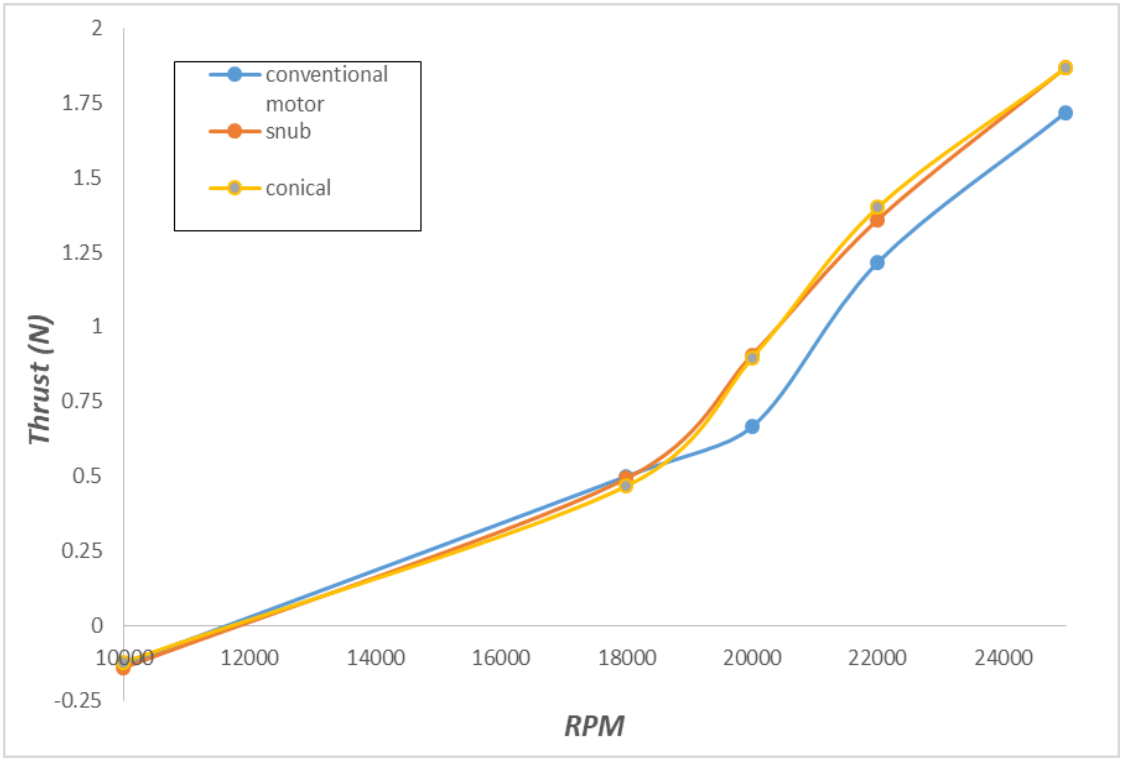

***Figure 13**: Total thrust as a function of RPM at 15 m/s*

***Figure 14**: Total drag as a function of RPM at 15 m/s*

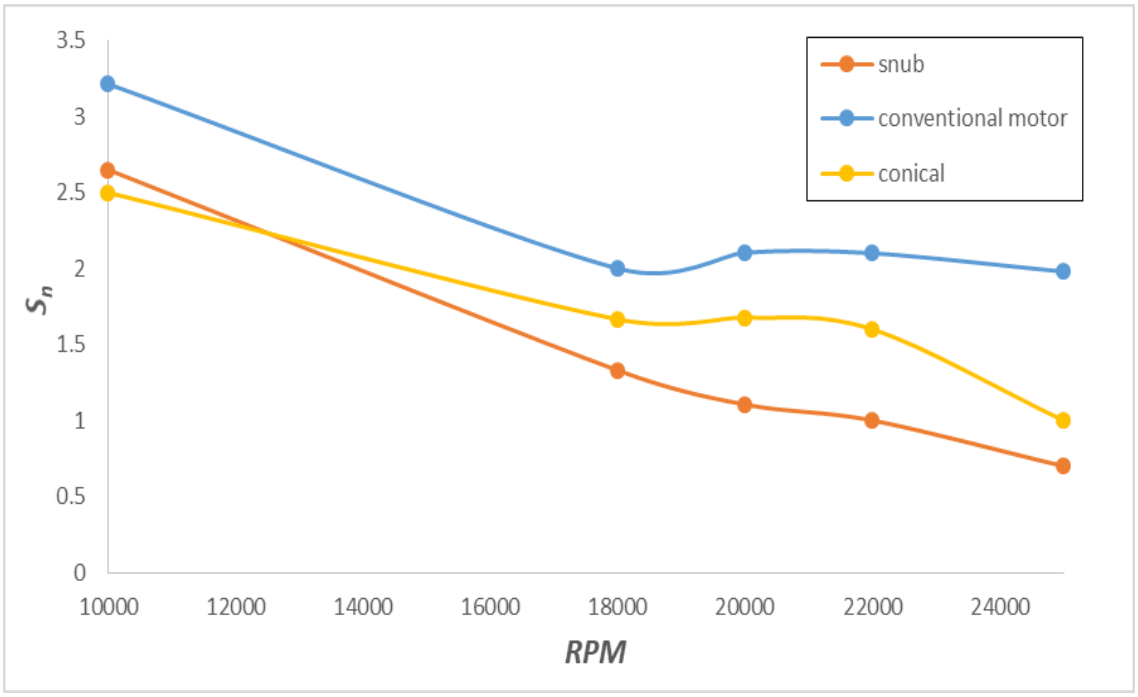

***Figure 15**: S_n as a function of RPM at 15 m/s*

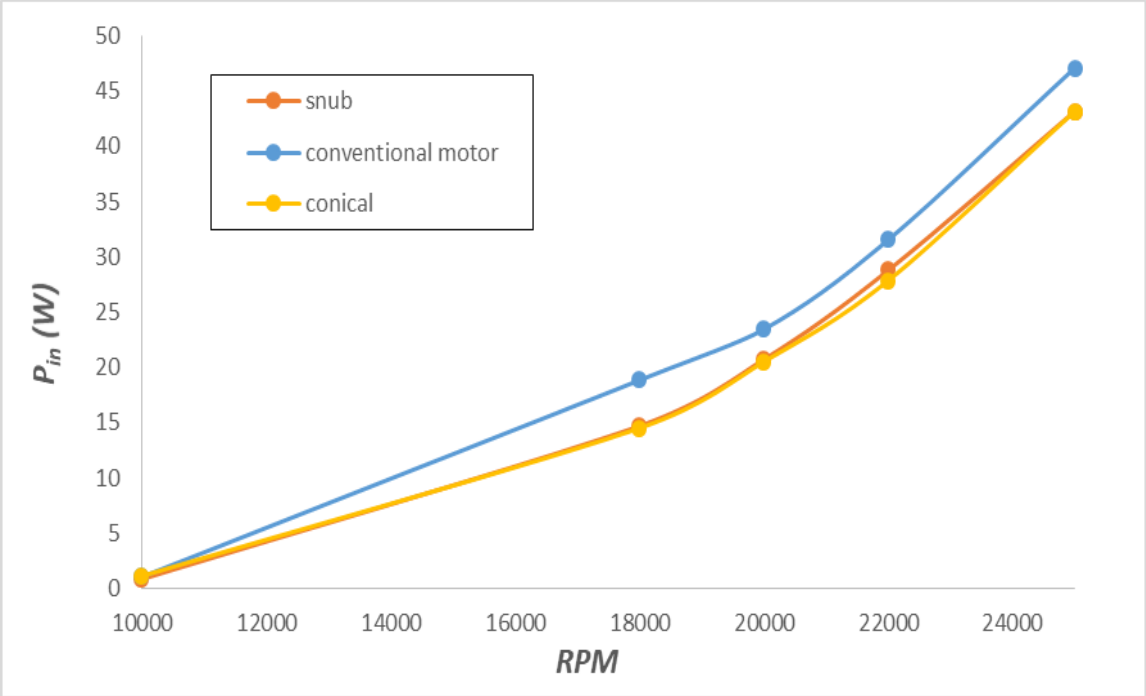

***Figure 16**: P_{in} as a function of RPM at 15 m/s*

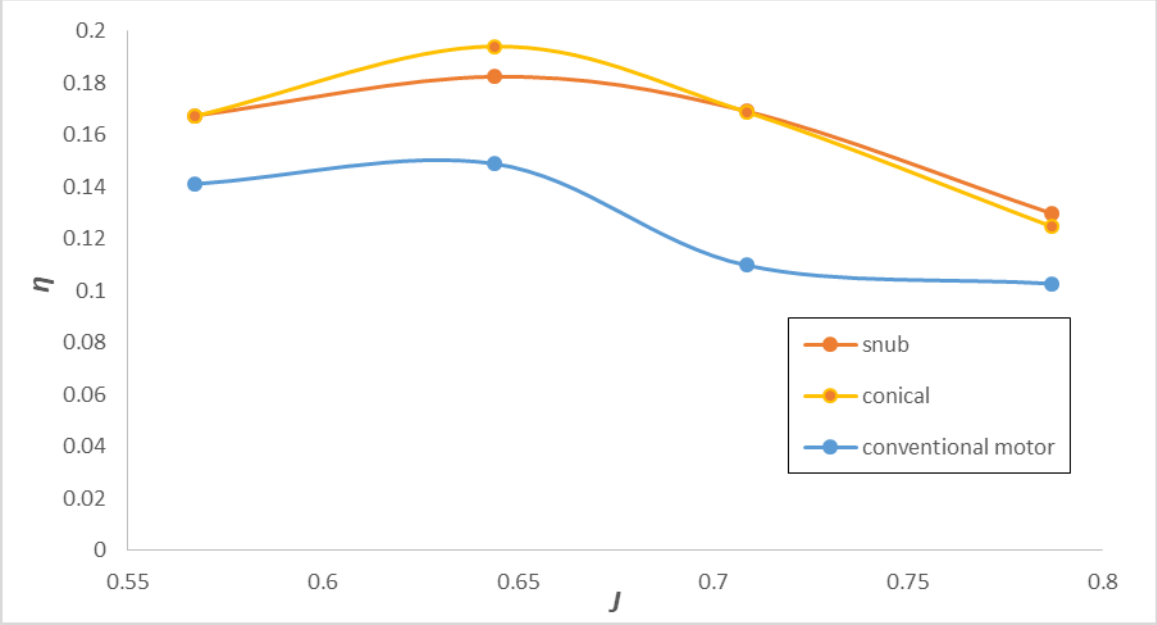

***Figure 17**: η as a function of J at 15 m/s*

From the *FEA* and *CFD* analysis above performed on the three configurations, it is evident that although both the snub and conical gearbox off-axis designs are comparable in terms of flow analysis, the conical gearbox design performs poorly in *FEA* with 5% more Von-Mises stress and visible stress concentration. It is therefore decided to select the off-axis snub gearbox ducted fan design and carry on with manufacturing and experimental analysis.

5. EXPERIMENTAL ANALYSIS

For the experimental wind tunnel analysis, the on-axis and off-axis snub gearbox configurations are 3d printed out of polished *sintered laser nylon 12.* The off-axis snub gearbox setup is presented in *Figure 19.*

***Figure 18**: Completed assembly: On-axis (left); Off-axis (right)*

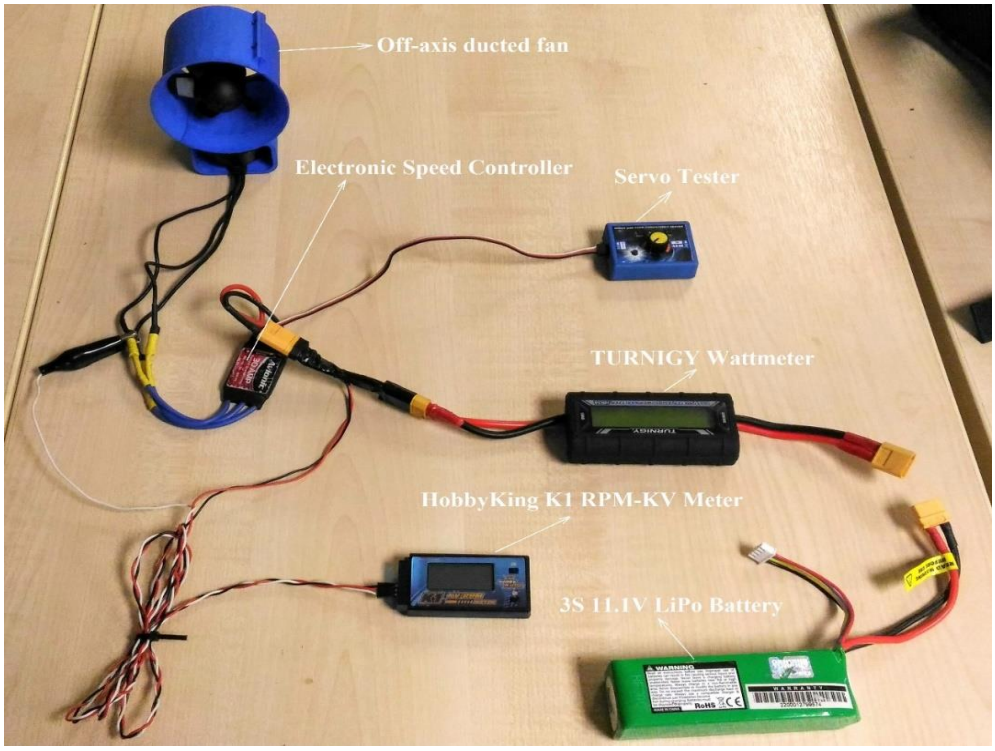

***Figure 19**: Typical circuit layout*

6. RESULTS AND DISCUSSION

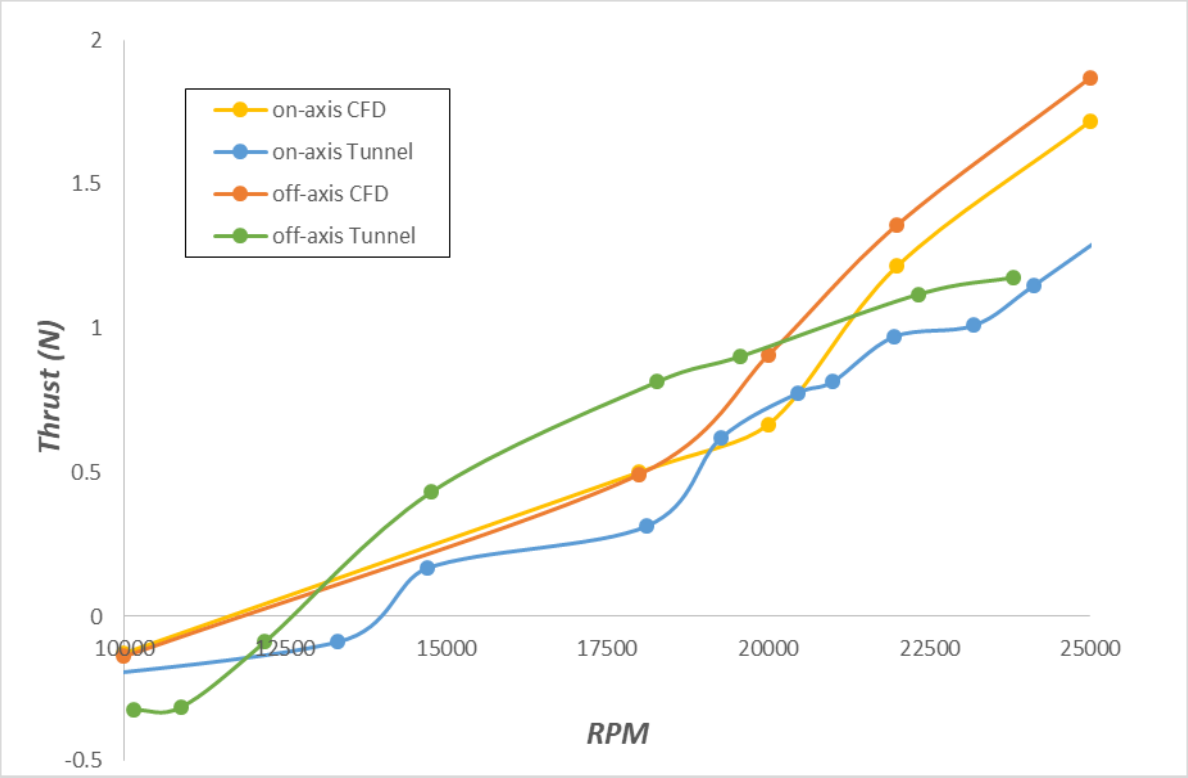

***Figure 20**: CFD and Tunnel Thrust comparison*

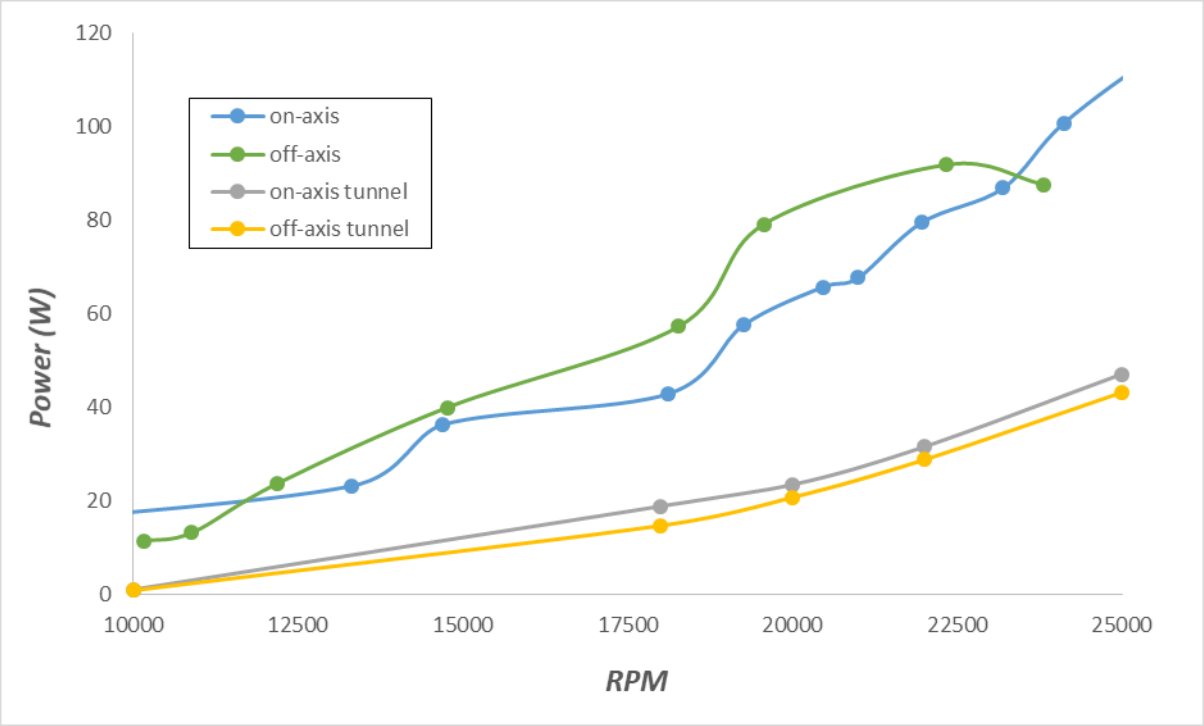

***Figure 21**: CFD and Tunnel Power comparison*

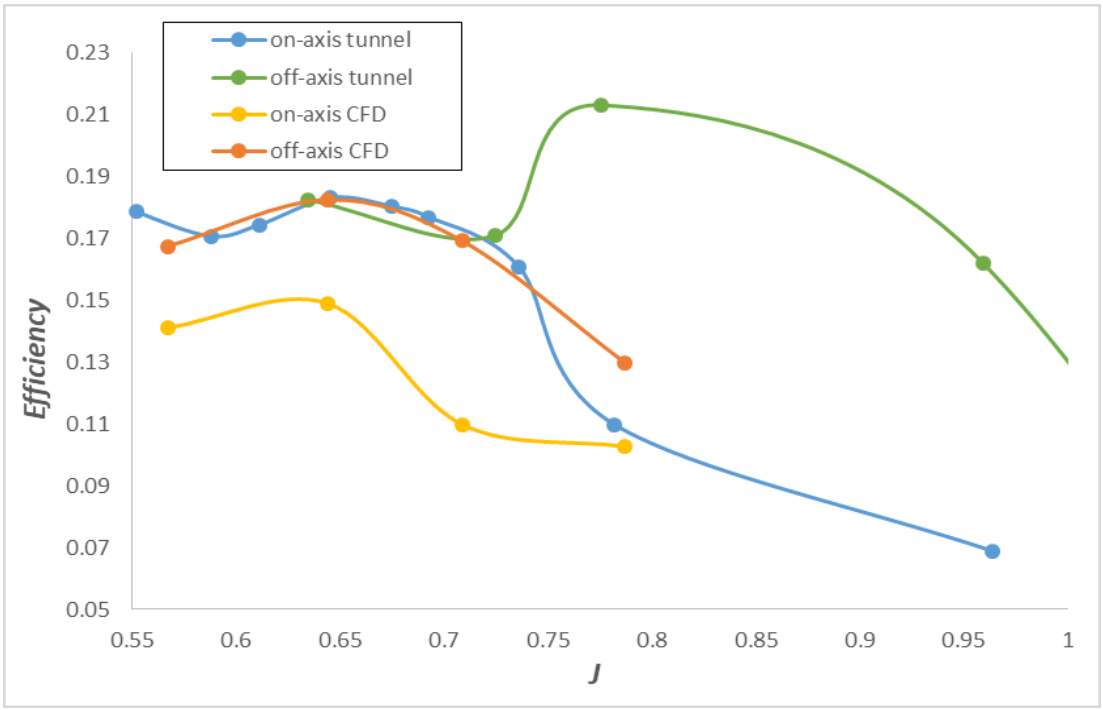

***Figure 22**: CFD and Tunnel efficiency comparison*

In order for the *CFD* and the experimental tunnel thrust results to be compared the tunnel thrust plots (*Figure 20)* are clipped to the range of 10000 through to 25000 *RPM.* The current *CFD* simulation is based on a pressure based solver and since upwards of 25000 *RPM* compressibility effect on blade tip becomes relevant, the simulations will become nonsensical. A very good agreement between both the simulations are found for both the on-axis and off-axis ducted fan designs. Although *CFD* plots are seen to overestimate thrust upwards of 22000 *RPM* but in general the comparison validates the *CFD* simulations. The off-axis in wind tunnel is found to perform best by producing approximately 50% more thrust between 15000 and 20000 *RPM,* however it gets limited thereafter owing to mechanical issues in the gearbox at high *RPM.*

Figure 21 illustrates the power comparison between the *CFD* and the wind tunnel simulations. The *CFD* plots correspond to the shaft power which ignores the mechanical losses like heat dissipation from bearings, friction between gears and heat dissipation from the motors used in both the cases. At an RPM of 24000 the power consumption in the tunnel simulation is observed to be approximately 50% more than that predicted by *CFD*. Here the off-axis in wind tunnel is found to consume almost similar amount of power compared to on-axis.

Figure 22 illustrates the efficiency comparison between the *CFD* and the wind tunnel simulations. A good agreement in off-axis plots between the *J* (advance ratio) of 0.63 through to 0.73 is found. However an agreement in the overall trend is found in on-axis plots, they are observed to converge towards *J* of 0.8. The off-axis in wind tunnel is best found to achieve an efficiency of over 50% between 0.75 *J* and 0.95 *J.*

REFERENCES

[1] Emma, "UAV Ducted Fan Nacelle: Design & Test", 2016

[2] Ignacio, "Design optimisation, build and test of a small scale ducted fan", 2016

[3] Robie, "Design and Construction of a Modular Ducted Fan Nacelle And Its Use to Test The Effect of Stator Design", 2017

[4] Nathan, "Design, Build and Validation of a UAV Propeller Test Rig", 2017

[5] Graf, "Effects of Duct Lip Shaping and Various Control Devices on the Hover and Forward Flight Performance of Ducted Fan UAVs", 2005

[6] Bardina, Huang and Coakley, "Turbulence Modelling Validation, Testing and Development", 1997

[7] Arturk and Camci, "Ducted Fan Inlet/Exit and Rotor Tip Flow Improvements for Vertical Lift Systems", 2010

[8] Arturk and Camci, "A Computational and Experimental Analysis of a Ducted Fan used in VTOL UAV Systems", 2011

[9] Arturk and Camci, "Experimental and Computational Assessment of a Ducted-Fan Rotor Flow Model", 2012

[10] Mort, "Performance Characteristics of a 4-Foot-Diameter Ducted Fan at Zero Angle of Attack for Several Fan Blade Angles", 1965

[11] Marcelo, Bruno, Newton and Jian, "Validation of Turbulence Models for Simulation of Axial Flow Compressor", 2009

[12] Eluchie, "Effect of Duct Lip Shaping and Drag Reduction on an Electrical Ducted Fan", 2016

[13] Konstantinos, "Ducted Tail Rotor Performance Prediction Using CFD", 2014

[14] Rezaeiha, Kalkman, Montazeri and Blocken, "Effect of the shaft on the aerodynamic performance of urban vertical axis wind turbines", 2017

[15] Petro, "Achieving High Electric Motor Efficiency", 2011

[16] Abrego and Bulaga, "Performance Study of a Ducted Fan System", 2002

[17] Abrego and Bulaga, "Performance Study and CFD Predictions of a Ducted Fan System", 2002

[18] Carlos, Jay and Eric, "Wind Turbine Tower Fairing Geometries to Decrease Shadow Effects", 2015

[19] Osgar, "Ducted Fan Aerodymanics and Modeling, with Applications of Steady and Synthetic Jet Flow Control", 2011

[20] Matt, "An Evaluation of Turbulence Models for the Numerical Study of Forced and Natural Convective Flow in Atria", 2009

[21] Wright Jr., "Ducted Fan Design", 2001

[22] 201831030633,"Off-Axis Motor Overdrive Ducted Fan", 2018.

[23] FEEG2001 UAV [Online] Available: https://www.southampton.ac.uk/courses/modules/feeg2001.page